



The PedS2/PedR2 Two-Component System Is Crucial for the Rare Earth Element Switch in *Pseudomonas putida* KT2440

Matthias Wehrmann,^a Charlotte Berthelot,^{b,c} Patrick Billard,^{b,c}  Janosch Klebensberger^a

^aUniversity of Stuttgart, Institute of Biochemistry and Technical Biochemistry, Stuttgart, Germany

^bUniversité de Lorraine, LIEC UMR7360, Faculté des Sciences et Technologies, Vandoeuvre-lès-Nancy, France

^cCNRS, LIEC UMR7360, Faculté des Sciences et Technologies, Vandoeuvre-lès-Nancy, France

ABSTRACT In *Pseudomonas putida* KT2440, two pyrroloquinoline quinone-dependent ethanol dehydrogenases (PQQ-EDHs) are responsible for the periplasmic oxidation of a broad variety of volatile organic compounds (VOCs). Depending on the availability of rare earth elements (REEs) of the lanthanide series (Ln^{3+}), we have recently reported that the transcription of the genes encoding the Ca^{2+} -utilizing enzyme PedE and the Ln^{3+} -utilizing enzyme PedH are inversely regulated. With adaptive evolution experiments, site-specific mutations, transcriptional reporter fusions, and complementation approaches, we now demonstrate that the PedS2/PedR2 (PP_2671/PP_2672) two-component system (TCS) plays a central role in the observed REE-mediated switch of PQQ-EDHs in *P. putida*. We provide evidence that in the absence of lanthanum (La^{3+}), the sensor histidine kinase PedS2 phosphorylates its cognate LuxR-type response regulator PedR2, which in turn not only activates *pedE* gene transcription but is also involved in repression of *pedH*. Our data further suggest that the presence of La^{3+} lowers kinase activity of PedS2, either by the direct binding of the metal ions to the periplasmic region of PedS2 or by an uncharacterized indirect interaction, leading to reduced levels of phosphorylated PedR2. Consequently, the decreasing *pedE* expression and concomitant alleviation of *pedH* repression causes—in conjunction with the transcriptional activation of the *pedH* gene by a yet unknown regulatory module—the Ln^{3+} -dependent transition from PedE- to PedH-catalyzed oxidation of alcoholic VOCs.

IMPORTANCE The function of lanthanides for methanotrophic and methylotrophic bacteria is gaining increasing attention, while knowledge about the role of rare earth elements (REEs) in nonmethylotrophic bacteria is still limited. The present study investigates the recently described differential expression of the two PQQ-EDHs of *P. putida* in response to lanthanides. We demonstrate that a specific TCS is crucial for their inverse regulation and provide evidence for a dual regulatory function of the LuxR-type response regulator involved. Thus, our study represents the first detailed characterization of the molecular mechanism underlying the REE switch of PQQ-EDHs in a nonmethylotrophic bacterium and stimulates subsequent investigations for the identification of additional genes or phenotypic traits that might be coregulated during REE-dependent niche adaptation.

KEYWORDS lanthanides, LuxR-type regulator, PQQ, PedR2, PedS2, *Pseudomonas putida*, dehydrogenases, histidine kinase, periplasm, rare earth element switch, signal transduction, two-component regulatory systems

In its natural soil habitat, *Pseudomonas putida* KT2440 is exposed to a broad range of potential carbon and energy sources (1–3), including plant-, fungus-, or bacterium-derived volatile organic compounds (VOCs) with alcohols or aldehydes as functional groups (4–6). For efficient capture and metabolism of such VOCs, *P. putida* makes use


Received 8 July 2018 Accepted 2 August 2018 Published 29 August 2018

Citation Wehrmann M, Berthelot C, Billard P, Klebensberger J. 2018. The PedS2/PedR2 two-component system is crucial for the rare earth element switch in *Pseudomonas putida* KT2440. *mSphere* 3:e00376-18. <https://doi.org/10.1128/mSphere.00376-18>.

Editor Craig D. Ellermeier, University of Iowa

Copyright © 2018 Wehrmann et al. This is an open-access article distributed under the terms of the [Creative Commons Attribution 4.0 International license](https://creativecommons.org/licenses/by/4.0/).

Address correspondence to Janosch Klebensberger, janosch.klebensberger@itb.uni-stuttgart.de.

 The two-component system PedS2/PedR2 is essential to orchestrate the rare earth element switch of PQQ-dependent ethanol dehydrogenases in the nonmethylotrophic organism *Pseudomonas putida* KT2440. @Klebensberger

of two pyrroloquinoline quinone (PQQ)-dependent ethanol dehydrogenases (PQQ-EDHs)—namely, PedE and PedH—to carry out the initial oxidation steps in the periplasm of the cell (7, 8). In a recent study, we found that these two type I quinoproteins (9, 10) exhibit a similar substrate scope but require different metal cofactors (8). In contrast to PedE, which uses Ca^{2+} ions, PedH was characterized as a rare earth element (REE)-dependent enzyme that relies on the presence of lanthanides (Ln^{3+}) for catalytic activity. Notably, due to their low solubility in most natural environments, REEs have long been considered to have no biological function (11). However, the discovery of the widespread occurrence of the REE-dependent XoxF type of PQQ-dependent methanol dehydrogenases (PQQ-MDHs), together with the more recent description of Ln^{3+} -dependent PQQ-EDHs, has highlighted the important role of REEs for many bacterial species in various environmental compartments (8, 12–20).

While in the absence of Ln^{3+} , the oxidation of methanol in methylotrophs is driven by Ca^{2+} -dependent PQQ-MDHs (MxaF type), the presence of small amounts of REE ions is usually sufficient to trigger a transcriptional switch to the XoxF type of PQQ-MDHs. This inverse regulation, called the REE switch, has been reported for many methanotrophic and/or methylotrophic organisms (13, 16, 21–24). From the growing number of studies, it has become apparent that the molecular mechanism underlying this switch for PQQ-MDHs is complex and can substantially differ among species. For example, the inverse regulation in the nonmethanotrophic methylotroph *Methylobacterium extorquens* strain AM1 is controlled by two different two-component systems (TCSs) (MxcQE and MxbDM) and the orphan response regulator MxaB (25–27). In this organism, it has been found that the transcriptional activation of both enzymes, the Ca^{2+} -dependent MxaF and the two Ln^{3+} -dependent XoxF1 and XoxF2, is entirely lost in a $\Delta\text{xoxF1} \Delta\text{xoxF2}$ double mutant (28). As a consequence, a complex regulation in which the different binding affinities of the *apo* form (no Ln^{3+} bound to the enzyme) and *holo* form (Ln^{3+} bound to the enzyme) of the XoxF proteins to the periplasmic domain of the sensor histidine kinase MxcQ is essential to regulate the switch was postulated (23).

The type I methanotroph *Methylomicrobium buryatense* strain 5GB1C is lacking homologues of the aforementioned TCS systems MxcQE and MxbDM (13). In this organism, the REE switch is regulated predominantly by the sensor histidine kinase MxaY (29). Chu and coworkers (29) found that the activation of MxaY in the absence of lanthanum activates transcription of the Ca^{2+} -dependent enzyme MxaF by a so-far-unknown response regulator. In addition, the deletion of MxaY was found to almost entirely eliminate the Ln^{3+} -mediated transcriptional activation of the Ln^{3+} -dependent enzyme XoxF in a partially MxaB-dependent manner that also results in a severe growth defect, both in the presence and absence of Ln^{3+} . As an additional layer of complexity, recent studies found that the presence of other metal ions such as copper, which is needed as a cofactor for the membrane-bound or particulate methane monooxygenase (pMMO) in methanotrophs, can significantly impact the REE-mediated switch (21, 22, 30).

In contrast to the increasing knowledge about the regulation of PQQ-MDHs in methylotrophs, the molecular basis underlying such a regulatory switch for PQQ-EDHs in nonmethylotrophic organisms is not established. In the present study, we identify the TCS encoded by PP_2671/PP_2672 (hereinafter referred to as PedS2/PedR2 according to the genetic nomenclature from Arias et al. [31]), consisting of the sensor histidine kinase PedS2 and its cognate LuxR-type transcriptional response regulator PedR2, as an essential regulatory module for the REE-mediated switch of PQQ-EDHs in *P. putida* KT2440. We provide evidence that the activity of PedS2 in the absence of lanthanides leads to phosphorylation of PedR2 (PedR2^P), which serves a dual regulatory function. On the one hand, PedR2^P acts as a strong transcriptional activator of the *pedE* gene, which is essential to allow growth with 2-phenylethanol in the absence of Ln^{3+} . At the same time, PedR2^P also functions as a repressor of *pedH*. From our data, we conclude that the presence of Ln^{3+} ions triggers a reduction in PedS2 activity, either by a direct binding of the metal to the periplasmic region of PedS2 or by an uncharacterized

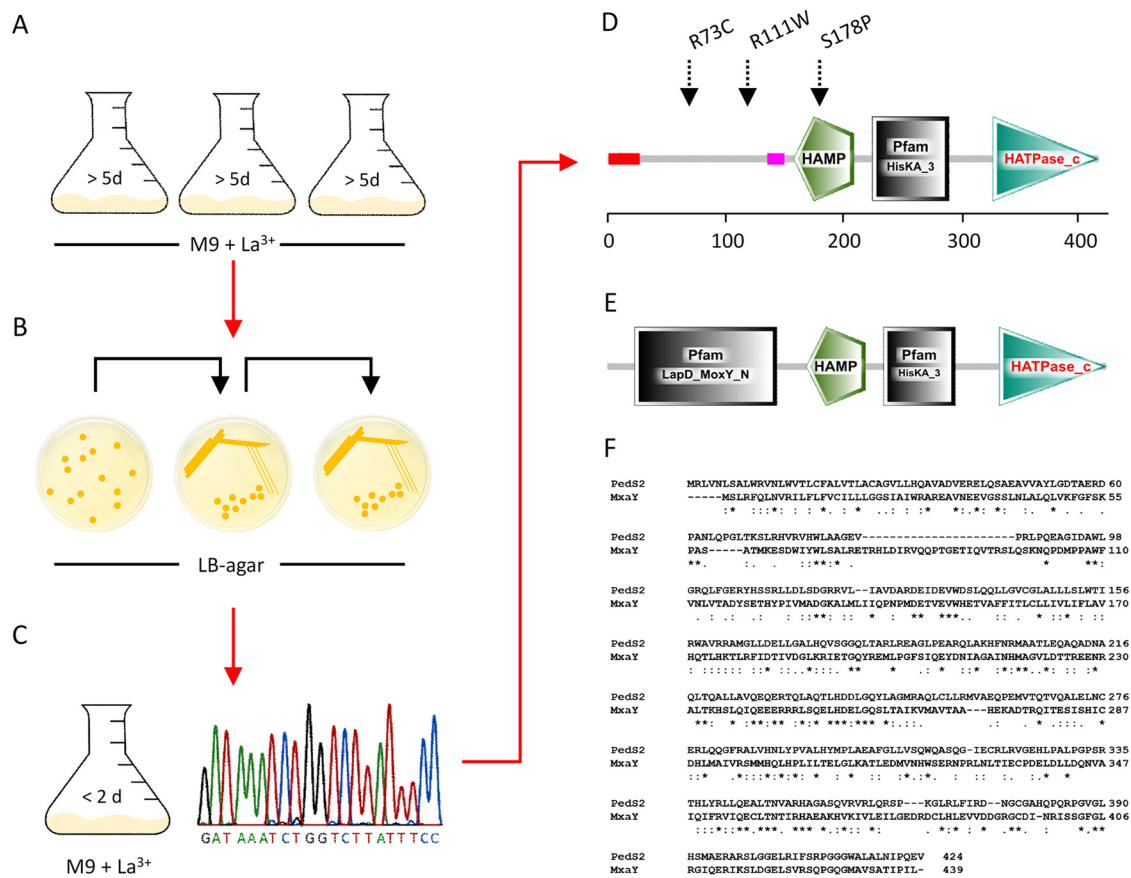


FIG 1 (A to D) Schemes of selection (A), clonal isolation (B), characterization and single nucleotide polymorphism (SNP) identification (C and D) in the two-component sensor histidine kinase PedS2 of the $\Delta pedH^{S1}$ (R73C), $\Delta pedH^{S2}$ (R111W), $\Delta pedH^{S3}$ (S178P) spontaneous mutants. (A) Cells of the $\Delta pedH$ strain were incubated in M9 medium supplemented with 5 mM 2-phenylethanol and 10 μ M $LaCl_3$ in plastic Erlenmeyer flasks ($n = 3$) at 30°C with shaking at 180 rpm. (B) After growth was observed (>5 days), dilutions from each culture were plated onto LB agar plates and incubated at 30°C. Individual clones were further streaked on LB agar twice prior to further characterization. (C) Clones were characterized for their growth behavior in M9 medium with 5 mM 2-phenylethanol in the presence of 10 μ M $LaCl_3$. Subsequently, one clone from each culture exhibiting faster growth than the parental $\Delta pedH$ strain was used for PCR amplification of the *pedS2* gene and multiple-sequence alignment analysis with the native sequence of the gene from the *Pseudomonas* Genome Database (52). (D and E) Visualization of domain composition of PedS2 of *P. putida* (D) and MxaY of *Methylomicrobium buryatense* 5GB1C (E) using the prediction from the Simple Modular Architecture Research Tool (53). (F) Amino acid sequence alignment of the PedS2 and MxaY proteins generated with Clustal Omega (50).

indirect interaction. This reduction of PedS2 activity, together with a proposed phosphatase activity of PedS2 under this condition, causes the accumulation of non-phosphorylated PedR2, which over time results in the loss of the regulatory activity of the protein, and facilitates—in concert with the positive-feedback function of PedH in the presence of Ln^{3+} ions—the switch between PedE- and PedH-dependent growth.

RESULTS

Identification of the sensor histidine kinase PedS2 as a lanthanide-responsive sensor. As a consequence of the inverse regulation of *pedE* and *pedH*, a *pedH* deletion strain does not grow within 48 h with 2-phenylethanol as the sole carbon source in the presence of a critical concentration of La^{3+} in the culture medium (8). To test whether strains can evolve to overcome the repression of *pedE* in the presence of Ln^{3+} , an adaptive evolution experiment was performed (see Fig. 1 for a general scheme).

When $\Delta pedH$ cultures were incubated with 2-phenylethanol in the presence of 10 μ M La^{3+} ions for longer than 5 days, growth was observed, indicating the occurrence of adapted strains (data not shown). When independent clones were isolated from such cultures and passaged several times on LB agar medium, their growth phenotype with 2-phenylethanol was much faster (<2 days) than that observed for

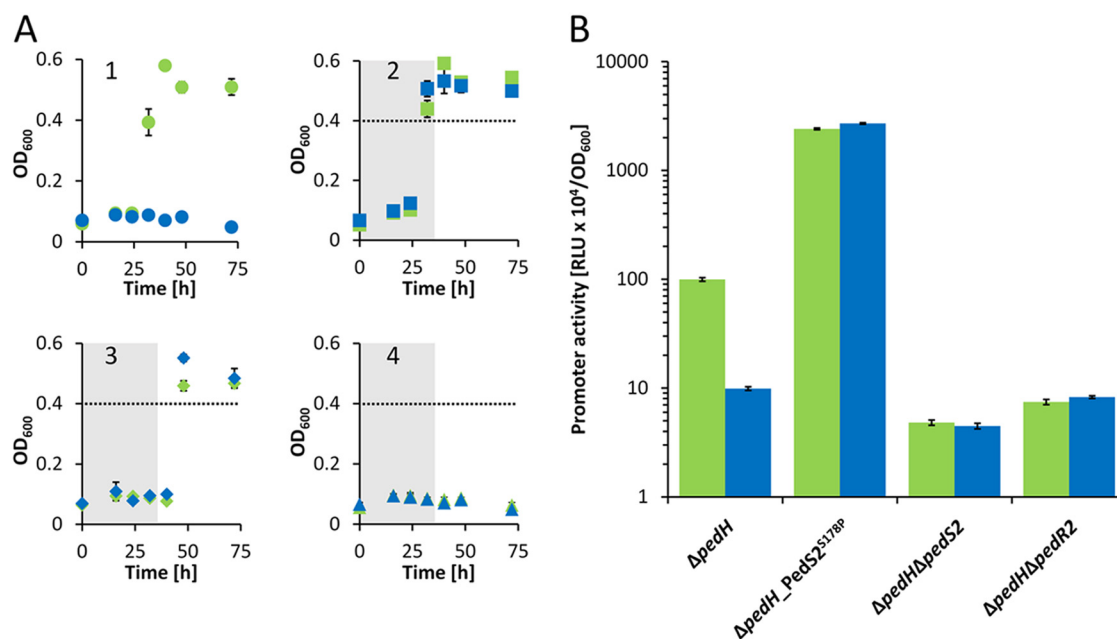


FIG 2 (A) Growth of $\Delta pedH$, $\Delta pedH_pedS2^{S178P}$, $\Delta pedH_pedS2$, and $\Delta pedH_pedR2$ strains. The $\Delta pedH$ (circles; panel 1), $\Delta pedH_pedS2^{S178P}$ (squares; panel 2), $\Delta pedH_pedS2$ (diamonds; panel 3), and $\Delta pedH_pedR2$ (triangles; panel 4) strains were grown at 30°C and 350 rpm shaking with M9 medium in 96-well plates supplemented with 5 mM 2-phenylethanol in the presence of 10 μ M La³⁺ (blue symbols) or in the absence of La³⁺ (green symbols). The gray areas in panels 2 to 4 show the time point by which the parental $\Delta pedH$ strain (circles) reached an OD₆₀₀ of >0.4 (dotted line). (B) Activities of the *pedE* promoter in $\Delta pedH$, $\Delta pedH_pedS2^{S178P}$, $\Delta pedH_pedS2$, and $\Delta pedH_pedR2$ strains in the presence (blue bars) or absence of La³⁺ (green bars) or measured in M9 medium supplemented with 1 mM 2-phenylethanol. Promoter activities are presented in relative light units (RLU × 10⁴) normalized to OD₆₀₀. All data represent the means for biological triplicates, and error bars correspond to the respective standard deviations.

their $\Delta pedH$ parental strain and very similar to the growth phenotype of the wild-type strain KT2440. Similar spontaneous suppressor mutants have been reported in methylotrophic organisms such as *Methylobacterium extorquens* strain AM1, *Methylomicrobium buryatense* strain 5GB1C, and *Methylobacterium aquaticum* strain 22A during growth with methanol (13, 16, 29). In *M. buryatense*, whole-genome sequencing revealed that the suppressor mutant strain was characterized by a mutation in the membrane-bound two-component sensor histidine kinase MxaY (29). In *Pseudomonas putida* KT2440, the gene *PP_2671* (hereinafter referred to as *pedS2*), located in close genomic proximity to *pedE* (*PP_2674*), encodes a membrane-bound histidine kinase sharing 25% amino acid sequence identity with MxaY (Fig. 1D to F). To test the hypothesis that mutations in *pedS2* are responsible for the emergence of suppressor phenotypes in the $\Delta pedH$ mutant strain during growth in the presence of La³⁺, the gene was sequenced in three individually isolated mutants ($\Delta pedH^{S1}$ to $\Delta pedH^{S3}$ mutant strains) (Fig. 1A to D). This analysis revealed that all strains contained a mutation in the *pedS2* sequence leading to a nonsynonymous substitution. These mutations were either located within a predicted periplasmic domain of unknown function (R73C [$\Delta pedH^{S1}$ strain] and R111W [$\Delta pedH^{S2}$ strain]) or within the HAMP domain (S178P [$\Delta pedH^{S3}$ strain]), which is responsible for signal transduction from the periplasm into the cytoplasm of the cell (32, 33). To verify that the identified mutations in *pedS2* are the primary cause of the suppressor phenotype, the S178P mutation from the $\Delta pedH^{S3}$ strain was introduced into the genetic background of the $\Delta pedH$ strain, resulting in the $\Delta pedH_pedS2^{S178P}$ strain.

In subsequent growth experiments with 2-phenylethanol in the absence of La³⁺, the $\Delta pedH$ and $\Delta pedH_pedS2^{S178P}$ mutants showed similar growth behavior with a lag phase of <32 h (Fig. 2A1 and A2). In the presence of 10 μ M La³⁺, however, the $\Delta pedH$ strain showed no growth within 72 h, whereas the $\Delta pedH_pedS2^{S178P}$ strain reached its maximum optical densities again after about 32 h of incubation, verifying that the

observed mutation in the histidine kinase *pedS2* gene was sufficient to cause the suppressor phenotype. We speculated that the LuxR-type response regulator *exaE* (*PP_2672*; hereinafter referred to as *pedR2*), which is located adjacent to *pedS2* within the genome of *P. putida* KT2440, represents the target of PedS2 activity. This assumption is based on the fact that PedR2 represents a homologue (65% amino acid sequence identity) of EraR (ExaE; PA1980), which forms a two-component system (TCS) with the cytosolic histidine kinase EraS (ExaD; PA1979) that activates expression of the *pedE* homologue *exaA* in *Pseudomonas aeruginosa* (34, 35). To test this hypothesis, *pedS2* as well as its potential cognate response regulator-encoding gene *pedR2*, were deleted in a $\Delta pedH$ background. In addition, strains suitable for probing promoter activity of *pedE* in $\Delta pedH$, $\Delta pedH_PedS2^{S178P}$, $\Delta pedH \Delta pedS2$, and $\Delta pedH \Delta pedR2$ mutant strains were constructed and subsequently analyzed during growth with 2-phenylethanol in the presence and absence of La^{3+} (Fig. 2B).

The PedS2/PedR2 TCS regulates *pedE* transcription in response to lanthanide availability. In accordance with the observed growth patterns, *pedE* promoter activities in the $\Delta pedH_PedS2^{S178P}$ mutant were almost identical in both the presence and absence of La^{3+} (ratio of *pedE* promoter activity in cells grown without La^{3+} to promoter activity in cells grown with $1 \mu M La^{3+}$, 0.89 ± 0.02) but increased more than 24-fold (24-fold \pm 1-fold and 27-fold \pm 1-fold, respectively) compared to the *pedE* promoter activities determined for cells of the $\Delta pedH$ strain grown in the absence of La^{3+} (Fig. 2B). The $\Delta pedH \Delta pedS2$ double mutant also showed a La^{3+} -independent growth phenotype similar to that of the $\Delta pedH_PedS2^{S178P}$ strain but with a clear delay (<48 h versus <32 h) (Fig. 2A3). Promoter activities for *pedE* were almost identical in this strain in the presence and absence of La^{3+} (ratio of *pedE* promoter activity in cells grown without La^{3+} to promoter activity in cells grown with $1 \mu M La^{3+}$, 1.07 ± 0.09) (Fig. 2B).

In contrast, incubations of 72 h (Fig. 2A4) or even prolonged incubations for more than 7 days (data not shown) did not result in detectable growth of the $\Delta pedH \Delta pedR2$ double mutant with 2-phenylethanol, both in the presence and absence of La^{3+} . Correspondingly, *pedE* promoter activities in this strain were low compared to those observed for cells of the $\Delta pedH$ strain in the presence of La^{3+} but in a range similar to those observed for the $\Delta pedH \Delta pedS2$ strain in the presence and absence of La^{3+} . These data demonstrate that the PedS2/PedR2 system is the predominant element in the La^{3+} -dependent regulation of *pedE* and that PedR2 is essential for PedE-dependent growth. However, as PedE-dependent growth can still be observed in the absence of PedS2 after prolonged incubations and in a PedR2-dependent manner (Fig. 2A3 and A4), we assume that at least one additional lanthanide-independent kinase must be able to phosphorylate PedR2, leading to transcriptional activation of *pedE* and functional production of the calcium-dependent enzyme under these conditions.

The PedS2/PedR2 TCS regulates the partial repression of *pedH* in the absence of lanthanides. On the basis of the critical role of PedS2/PedR2 in the regulation of *pedE* and the fact that LuxR-type regulators have been demonstrated to be capable of acting as both transcriptional activators and repressors (36, 37), we speculated that this TCS could also be involved in the regulation of *pedH*. To test this hypothesis, $\Delta pedE_PedS2^{S178P}$, $\Delta pedE \Delta pedS2$, and $\Delta pedE \Delta pedR2$ mutant strains were generated, and a transcriptional reporter suitable for probing *pedH* promoter activities was integrated into the genome of each of these strains.

Experiments with 2-phenylethanol revealed that $\Delta pedE$, $\Delta pedE \Delta pedS2$, and $\Delta pedE \Delta pedR2$ mutant strains showed La^{3+} -dependent growth after a lag phase of <24 h and reached the maximum optical density at 600 nm (OD_{600}) after ≤ 32 h (Fig. 3A1, A3, and A4). In contrast, the $\Delta pedE_PedS2^{S178P}$ strain exhibited an extended lag phase (>24 h) and consistently reached the maximum OD_{600} only after prolonged incubations (≥ 32 h [Fig. 3A2]). In accordance with these growth results, the *pedH* promoter activities of $\Delta pedE$, $\Delta pedE \Delta pedS2$, and $\Delta pedE \Delta pedR2$ strains were in a similar range, whereas *pedH* promoter activities in the $\Delta pedE_PedS2^{S178P}$ strain were 45-fold \pm 2-fold and 30-fold \pm 2-fold lower than the promoter activities of the $\Delta pedE$ strain in the absence or presence

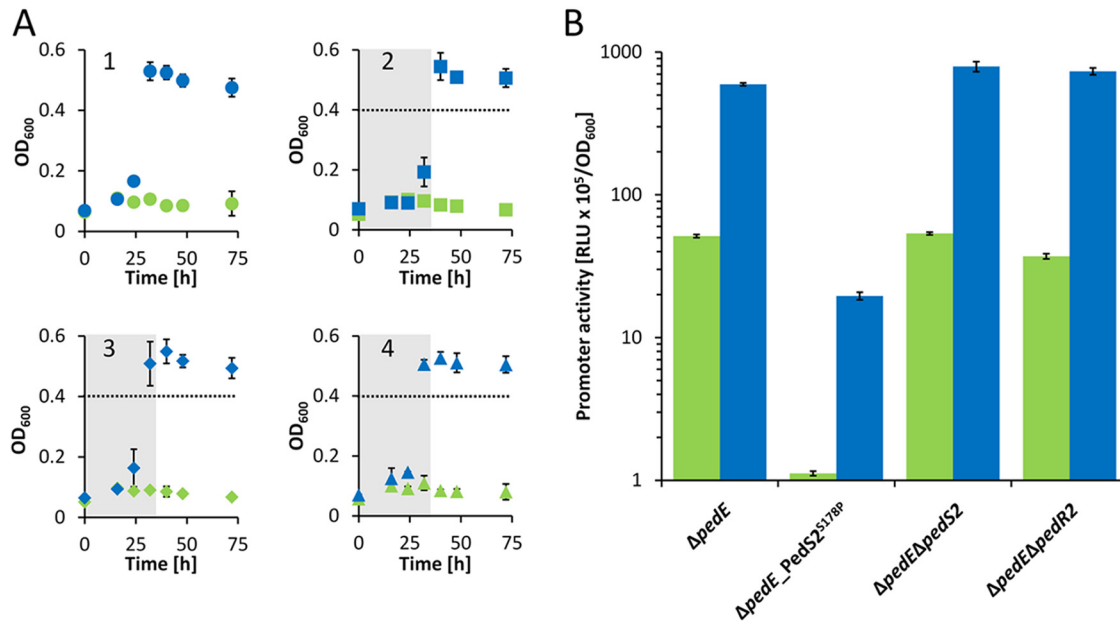


FIG 3 (A) Growth of *ΔpedE*, *ΔpedE_PedS2^{S178P}*, *ΔpedE ΔpedS2*, and *ΔpedE ΔpedR2* strains. The *ΔpedE* (circles; panel 1), *ΔpedE_PedS2^{S178P}* (squares; panel 2), *ΔpedE ΔpedS2* (diamonds; panel 3), and *ΔpedE ΔpedR2* (triangles; panel 4) were grown at 30°C and 350 rpm shaking with M9 medium in 96-well plates supplemented with 5 mM 2-phenylethanol in the presence of 10 μM La³⁺ (blue symbols) or absence of La³⁺ (green symbols). The gray areas in panels 2 to 4 show the time point by which the parental *ΔpedE* strain (circles) reached their maximum OD₆₀₀. (B) Activities of the *pedH* promoter in *ΔpedE*, *ΔpedE_PedS2^{S178P}*, *ΔpedE ΔpedS2*, and *ΔpedE ΔpedR2* strains in the presence of 1 μM La³⁺ (blue bars) or in the absence of La³⁺ (green bars) or measured in M9 medium supplemented with 1 mM 2-phenylethanol. Promoter activities are presented in relative light units (RLU × 10⁵) normalized to OD₆₀₀. All data represent the means for biological triplicates, and error bars correspond to the respective standard deviations.

of La³⁺, respectively (Fig. 3B). Assuming that the S178P mutation in PedS2 results in a sensor kinase activity that mimics that of the wild-type protein in the absence of lanthanides, it is very likely that PedS2 is responsible for the repression of *pedH* under the La³⁺-free conditions leading to the observed delay in growth. To find out whether this regulatory effect on *pedH* proceeds via the response regulator PedR2, as is the case for *pedE*, or is caused by an unknown additional target of PedS2, the *ΔpedE_PedS2^{S178P} ΔpedR2* triple mutant strain was generated and characterized for its growth phenotype (Fig. 4A). In this experiment, the *ΔpedE* and *ΔpedE_PedS2^{S178P}* strains both grew with 2-phenylethanol but with clear differences in the corresponding lag phases and maximum growth rates ($0.087 \pm 0.003 \text{ h}^{-1}$ versus $0.057 \pm 0.001 \text{ h}^{-1}$), confirming the previous results from growth in 96-well plates (Fig. 3A). In contrast, the additional deletion of the response regulator PedR2 eliminated the growth defect caused by the PedS2^{S178P} allele, leading to a growth behavior of the *ΔpedE_PedS2^{S178P} ΔpedR2* strain (Fig. 4A), which was indistinguishable (maximum growth rate, $0.089 \pm 0.003 \text{ h}^{-1}$) from that of the *ΔpedE* strain.

The conserved phosphorylation site D53 in PedR2 is essential for the REE-mediated switch. In order to study the essentiality of the phosphorylation site at position D53 of PedR2 (38, 39), we used inducible low-copy-number constructs for the production of the wild-type PedR2 protein (pJEM[PedR2]) and a mutated variant, in which the conserved aspartate in the CheY-like receiver domain was replaced by an alanine (pJEM[PedR2^{D53A}]). After transformation of these plasmids into the *ΔpedH ΔpedR2* and *ΔpedE_PedS2^{S178P} ΔpedR2* mutant strains, their growth with 2-phenylethanol in the presence and absence of La³⁺ was monitored. When the plasmid-borne wild-type regulator PedR2 was induced in cells of the *ΔpedH ΔpedR2* strain, growth was observed after a lag phase of <24 h (maximum growth rate, $0.032 \pm 0.005 \text{ h}^{-1}$), whereas the PedR2^{D53A} variant was unable to restore PedE-dependent growth in the same strain (Fig. 4B). Intriguingly, the reverse result was obtained in the *ΔpedE_PedS2^{S178P} ΔpedR2* strain. Here, the PedR2^{D53A} variant allowed PedH-dependent

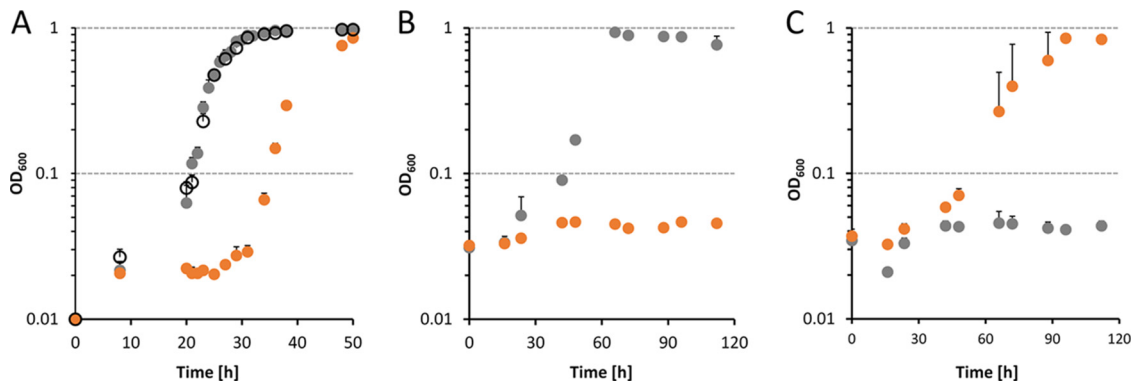


FIG 4 Growth of different *P. putida* strains at 30°C and 180 rpm shaking with M9 medium in polycarbonate Erlenmeyer flasks supplemented with 5 mM 2-phenylethanol and 10 μ M La^{3+} in the absence (A) and presence of kanamycin (B and C) for plasmid maintenance. Flasks were inoculated at an OD_{600} of 0.01 (A) or 0.03 (B and C) with washed cells from M9 overnight cultures grown with succinate in the absence (A) or presence (B and C) of kanamycin and 0.2% (wt/vol) rhamnose to induce pJEM[PedR2] and pJEM[PedR2^{D53A}] plasmids. (A) Growth of $\Delta pedE$ (black circles), $\Delta pedE_PedS2^{5178P}$ (orange circles), and $\Delta pedE_PedS2^{5178P} \Delta pedR2$ (gray circles) strains. (B) Growth of $\Delta pedH_PedS2^{5178P} \Delta pedR2$ strain harboring pJEM[PedR2] (gray circles) or pJEM[PedR2^{D53A}] (orange circles). (C) Growth of $\Delta pedE_PedS2^{5178P} \Delta pedR2$ strain harboring pJEM[PedR2] (gray circles) or pJEM[PedR2^{D53A}] (orange circles). Data points represent the means for biological triplets, and error bars correspond to the respective standard deviations (positive error values).

growth (maximum growth rate, $0.026 \pm 0.002 \text{ h}^{-1}$), whereas the wild-type regulator PedR2 did not lead to significant growth within 120 h of incubation (Fig. 4C).

DISCUSSION

We recently demonstrated that in *P. putida* KT2440, the production of the two PQQ-EDHs PedE and PedH is both tightly and inversely regulated depending on lanthanide availability, representing the first reported REE switch for PQQ-EDHs in a nonmethylotrophic organism (8). In this study, we were able to show that Ln^{3+} -dependent transcriptional activation of *pedH* is mostly, but not entirely, dependent on the presence of the PedH protein itself by a so-far unknown mechanism and transcriptional regulator (Fig. 5A). Notably, the Ln^{3+} -dependent transcriptional repression of *pedE* remained elusive. In the current study, we present a detailed characterization of the mechanism underlying PedE and PedH regulation, in which the PedS2/PedR2 TCS acts as an essential signaling module for the REE-mediated switch between the two quinoproteins.

Similar to the recently characterized spontaneous mutant of *M. buryatense* (29), we found that a single nonsynonymous mutation within the periplasmic region of the sensor histidine kinase PedS2 (PedS2^{5178P}), which differs from the LapD/MoxY domain found in MxaY of *M. buryatense* (Fig. 1), is sufficient to terminate the Ln^{3+} -mediated repression of *pedE*. Notably, various mutations at different sites of the protein can cause the observed suppressor phenotype. This might explain the repeated and fast occurrence of these suppressor mutants in our experiments and would support a similar notion in *M. buryatense* (13, 29).

Besides the essentiality for *pedE* regulation, our experimental data further provide strong evidence that PedS2 is also involved in the repression of *pedH* in the absence of lanthanides, but not in its Ln^{3+} -dependent activation. This is based on the observation that the $\Delta pedE \Delta pedS2$ deletion strain did not show any differences in growth and *pedH* activation, while the $\Delta pedE_PedS2^{5178P}$ suppressor mutant displayed decreased *pedH* promoter activity and a strongly increased lag phase in growth experiments in the presence of La^{3+} . The complementation assay with the inducible PedR2 variants further demonstrates that the *pedS2*-dependent regulation of *pedE* and *pedH* is mediated by the LuxR-type response regulator PedR2 for both genes. From these data, we conclude that in the absence of La^{3+} ions, the PedS2 sensor histidine kinase is active and triggers phosphorylation of PedR2 at the conserved position D53 (PedR2^P) (38, 39). The phosphorylated state of PedS2 subsequently has a dual regulatory function, namely, the

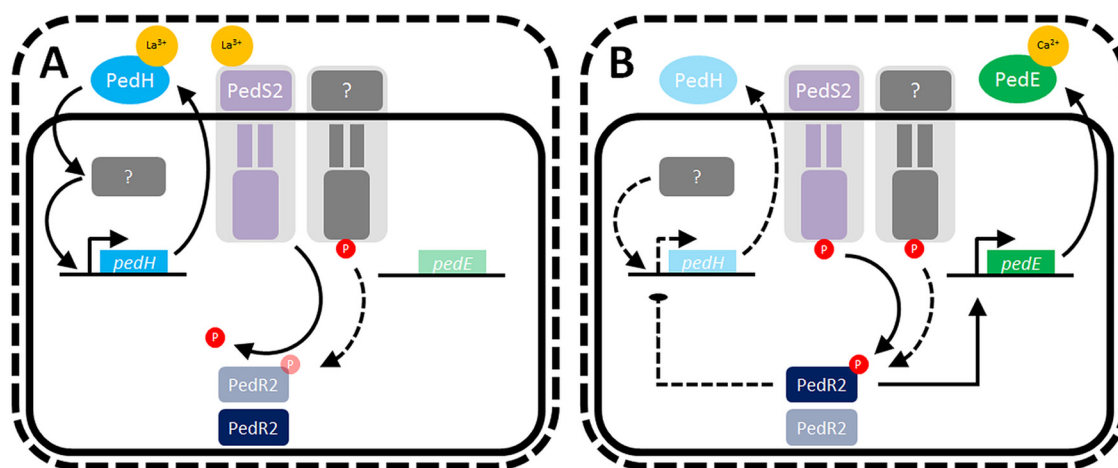


FIG 5 Working hypothesis of rare earth element (REE)-mediated switch of *pedE* and *pedH* in *Pseudomonas putida* KT2440. (A) The presence of REEs in the medium leads to binding of Ln^{3+} ions to PedH and the periplasmic domain of PedS2. The binding to PedH leads to the catalytic activation of the enzyme and triggers enhanced transcriptional activation of *pedH* by a so-far unknown mechanism and regulator, which is indicated by a gray box (8). Binding to the periplasmic domain of PedS2 leads to an outside-in signaling via the HAMP domain and decreases the kinase activity of the protein toward its cognate response regulator PedR2. In addition, this state of the PedS2 sensor is believed to exhibit phosphatase activity to reduce cross talk of an unidentified kinase (indicated by a gray membrane-bound protein) with activity toward PedR2 (for a more detailed explanation, see the text). (B) In the absence of REEs, the sensor kinase PedS2 is active and phosphorylates the cognate response regulator PedR2 at position D53. The phosphorylated PedR2 has a dual regulatory function as a strong *pedE* activator and a repressor of *pedH*. Black lines indicate known regulations or functionalities. Solid lines indicate a strong regulatory effect on genes or production of enzymes, whereas dotted lines indicate weaker regulatory effects or low production of enzymes.

activation of *pedE* and concomitant repression of *pedH* transcription (Fig. 5A). In this context, it is interesting to note that expression of the *exaA* gene in *Azospirillum brasilense* Sp7, which encodes a pyrroloquinoline quinone (PQQ)-dependent alcohol dehydrogenase, is dependent on σ^{54} and its interaction with a LuxR-type response regulator that shares 45% sequence identity with PedR2 (40). Whether the transcriptional activation of *pedE* is dependent on a similar interaction of PedR2 with a specific sigma factor is currently unknown.

To our surprise, a strain lacking PedS2 ($\Delta pedH \Delta pedS2$ strain) was still able to grow on 2-phenylethanol in the absence of Ln^{3+} , even though it exhibited an increased lag phase and low *pedE* promoter activities (Fig. 2A3). As our study provides strong evidence that phosphorylation of PedR2 is essential for transcriptional activation of *pedE*, this observation indicates that an additional so-far unidentified kinase beside PedS2 is capable of phosphorylating PedR2 to facilitate growth of this strain under these conditions (indicated in Fig. 5 as a gray membrane-bound protein). Given that such an additional kinase exists, it is even more surprising that a *pedH* single mutant, in contrast to the aforementioned $\Delta pedH \Delta pedS2$ double mutant, is able to grow in the presence of REEs only when PedS2 is mutated (e.g., PedS2^{S178P} [Fig. 2A1]). This suggests that the activity of the additional kinase toward PedR2 in the presence of La^{3+} is repressed as long as PedS2 is functional. As an intrinsic phosphatase activity has been found for many bacterial sensory histidine kinases (33, 41, 42), we hence propose that PedS2 also exhibits phosphatase activity on PedR2^P in the presence of La^{3+} , thereby ensuring specificity of the signal transduction pathway and eliminating interference from other nonspecific kinases. In our working hypothesis, the presence of lanthanides in the medium leads to the repression of PedS2 kinase activity, most likely by direct binding of the metal ions to its periplasmic domain. The reduced kinase activity and postulated phosphatase activity of PedS2 in the presence of Ln^{3+} consequently leads to the accumulation of unphosphorylated PedR2, which finally results in the loss of its regulatory functions. In addition, the transcription of *pedH* is activated via a yet unknown pathway, in which a functional PedH protein is an essential component, most likely by acting as a lanthanide sensor (8).

TABLE 1 Bacterial strains and plasmids used in this study

Bacterial strain or plasmid	Relevant feature(s)	Reference
Bacterial strains		
KT2440	Wild-type strain of <i>Pseudomonas putida</i> (ATCC 47054)	
KT2440*	KT2440 with a markerless deletion of <i>upp</i> ; parent strain for deletion mutants	48
$\Delta pedE$	KT2440* with a markerless deletion of <i>pedE</i>	7
$\Delta pedE \Delta pedS2$	$\Delta pedE$ strain with a markerless deletion of <i>pedS2</i> (PP_2671)	This study
$\Delta pedE \Delta pedR2$	$\Delta pedE$ strain with a markerless deletion of <i>pedR2</i> (PP_2672)	This study
$\Delta pedE_PedS2^{S178P}$	$\Delta pedE$ strain with S178P mutation in <i>PedS2</i>	This study
$\Delta pedE_PedS2^{S178P} \Delta pedR2$	$\Delta pedE_PedS2^{S178P}$ strain with a markerless deletion of <i>pedR2</i>	This study
$\Delta pedH$	KT2440* with a markerless deletion of <i>pedH</i>	7
$\Delta pedH \Delta pedS2$	$\Delta pedH$ strain with a markerless deletion of <i>pedS2</i>	This study
$\Delta pedH \Delta pedR2$	$\Delta pedH$ strain with a markerless deletion of <i>pedR2</i>	This study
$\Delta pedH_PedS2^{S178P}$	$\Delta pedH$ strain with S178P mutation <i>PedS2</i>	This study
$\Delta pedH_PedS2^{S178P} \Delta pedR2$	$\Delta pedH_PedS2^{S178P}$ strain with a markerless deletion of <i>pedR2</i>	This study
<i>E. coli</i> BL21(DE3)	F ⁻ <i>ompT gal dcm lon hsdSB</i> (r _B ⁻ m _B ⁻) λ (DE3 [<i>lacI lacUV5-T7 gene 1 ind1 sam7 nin5</i>])	
<i>E. coli</i> DH5 α	<i>fhuA2 lac</i> (del)U169 <i>phoA glnV44 ϕ80' lacZ</i> (del)M15 <i>gyrA96 recA1 relA1 endA1 thi-1 hsdR17</i>	
KT2440*:: <i>Tn7-pedE-lux</i>	KT2440* with insertion of miniTn7- <i>pedE-lux</i>	8
KT2440*:: <i>Tn7-pedH-lux</i>	KT2440* with insertion of miniTn7- <i>pedH-lux</i>	8
$\Delta pedE$:: <i>Tn7-pedE-lux</i>	$\Delta pedE$ strain with insertion of miniTn7- <i>pedE-lux</i>	8
$\Delta pedE$:: <i>Tn7-pedH-lux</i>	$\Delta pedE$ strain with insertion of miniTn7- <i>pedH-lux</i>	8
$\Delta pedH$:: <i>Tn7-pedE-lux</i>	$\Delta pedH$ strain with insertion of miniTn7- <i>pedE-lux</i>	8
$\Delta pedH$:: <i>Tn7-pedH-lux</i>	$\Delta pedH$ strain with insertion of miniTn7- <i>pedH-lux</i>	8
$\Delta pedE \Delta pedS2$:: <i>Tn7-pedH-lux</i>	$\Delta pedE \Delta pedS2$ strain with insertion of miniTn7- <i>pedH-lux</i>	This study
$\Delta pedE \Delta pedR2$:: <i>Tn7-pedH-lux</i>	$\Delta pedE \Delta pedR2$ strain with insertion of miniTn7- <i>pedH-lux</i>	This study
$\Delta pedE_PedS2^{S178P}$:: <i>Tn7-pedH-lux</i>	$\Delta pedE_PedS2^{S178P}$ strain with insertion of miniTn7- <i>pedH-lux</i>	This study
$\Delta pedH \Delta pedS2$:: <i>Tn7-pedE-lux</i>	$\Delta pedH \Delta pedS2$ strain with insertion of miniTn7- <i>pedE-lux</i>	This study
$\Delta pedH \Delta pedR2$:: <i>Tn7-pedE-lux</i>	$\Delta pedH \Delta pedR2$ strain with insertion of miniTn7- <i>pedE-lux</i>	This study
$\Delta pedH_PedS2^{S178P}$:: <i>Tn7-pedE-lux</i>	$\Delta pedH_PedS2^{S178P}$ strain with insertion of miniTn7- <i>pedE-lux</i>	This study
Plasmids		
pJeM1	Rhamnose-inducible vector (pBBR1MCS backbone) with low copy number	51
pJOE6261.2	Suicide vector for gene deletions	48
pMW55	pJOE6261.2-based deletion vector for gene <i>PP_2671</i>	This study
pMW56	pJOE6261.2-based vector for introducing the S178P mutation in <i>PedS2</i>	This study
pMW61	pJOE6261.2-based deletion vector for gene <i>PP_2672</i>	This study
pUC18-mini-Tn7T- <i>pedE-lux-Gm</i>	pUC18-mini-Tn7T- <i>Gm-lux</i> vector with the promoter of <i>pedE</i> driving transcription of <i>luxCDABE</i>	8
pUC18-mini-Tn7T- <i>pedH-lux-Gm</i>	pUC18-mini-Tn7T- <i>lux-Gm</i> vector with the promoter of <i>pedH</i> driving transcription of <i>luxCDABE</i>	8
pTNS2	Helper plasmid for Tn7 integration	49
pJEM[<i>PedR2</i>]	Rhamnose-inducible induction of <i>PedR2</i>	This study
pJEM[<i>PedR2</i> ^{D53A}]	Rhamnose-inducible induction of <i>PedR2</i> ^{D53A}	This study

In conclusion, it appears that the REE-mediated switches in *Methylobacterium extorquens* AM1 and *Methylomicrobium buryatense* during growth with methanol are predominantly dependent on only one lanthanide-responsive pathway, which either proceeds via the XoxF1 and XoxF2 proteins or via the MxaY protein (23, 29). Our results establish that in *P. putida* KT2440, a combination of at least two independent pathways are important to orchestrate the inverse regulation of *pedE* and *pedH* in response to lanthanides efficiently.

Several recent studies suggest that in methano- and methylotrophic bacteria, the REE switch might affect more genes than only the genes needed for the periplasmic oxidation system itself (16, 22, 43). Reports on physiological consequences are, however, inconsistent as some studies found no effects (13, 16, 23, 44), whereas other studies reported a stimulating effect on biofilm formation, growth rates, and overall yields in the presence of REE (43, 45). We think it is not unlikely that additional REE-mediated regulatory effects also exist in *P. putida* KT2440 in a context-dependent manner. Thus, one of our current foci is to investigate the global regulatory impact and physiological consequences of the presence and absence of lanthanides under various environmental conditions.

MATERIALS AND METHODS

Bacterial strains, plasmids, and culture conditions. A detailed description of the bacterial strains, plasmids, and primers used in this study can be found in Tables 1 and 2. If not stated otherwise,

TABLE 2 Primers used in this study

Primer	Primer sequence (5' → 3')	Annealing temp (°C)
MWH85	GGAAATATGCAGAAAGTAGCGCTCG	60
MWH86	TCITCACCCTGGCGGCCT	60
MWH90	GCCGCTTTGGTCCCGCAGGCACTGGCTGCTGC	60
MWH91	CGATATCAAAGCGGTTCTCCTCAGGC	60
MWH92	GAACCGCTTTGAATATCGTGTGGTGCATGACCAC	60
MWH93	GCAGGTGCGACTCTAGAGGATGCACAAGCTCGGCG	60
MWH98	GCCGCTTTGGTCCCGAGGTAGTAATTCAGTCCGGGGG	60
MWH99	TGCCCGCCTGGGACCTGGTG	60
MWH100	GGTCCCAGGCGGCAATTG	60
MWH101	GCAGGTGCGACTCTAGAGGCGCCATTGTCGCGAATG	60
MWH106	GCCGCTTTGGTCCCGGCGAGGAGCAGGAGCGTAC	65
MWH107	TGAAATACCCACACTCTCGGGGAATGTTAAG	65
MWH108	GGAGGTGTGGGTATTTCATTGCACCTGTTGGGGC	65
MWH109	GCAGGTGCGACTCTAGAGGAGCCAACCTGACCC	65

Escherichia coli and *Pseudomonas putida* KT2440 strains were maintained on solidified LB medium. Routinely, strains were cultured in liquid LB medium (46) or a modified M9 salt medium (8) supplemented with 25 mM succinate or 5 mM 2-phenylethanol as a source of carbon and energy at 30°C and shaking, if not stated otherwise. For maintenance and selection, 40 µg ml⁻¹ kanamycin or 15 µg ml⁻¹ gentamicin for *E. coli* or 40 µg ml⁻¹ kanamycin, 20 µg ml⁻¹ 5-fluorouracil, or 15 µg ml⁻¹ gentamicin for *P. putida* strains was added to the medium, if indicated.

Liquid medium growth experiments. All liquid growth experiments were carried out using modified M9 medium with 25 mM succinate or 5 mM 2-phenylethanol as the sole source of carbon and energy (see above) in 125-ml or 250-ml polycarbonate Erlenmeyer flasks (Corning) or in 96-well 2-ml deep-well plates (Carl Roth) as described previously (8). Briefly, washed cells from overnight cultures grown with succinate at 30°C and 180 rpm shaking were used to inoculate fresh medium with an optical density at 600 nm (OD₆₀₀) of 0.01 and incubated at 30°C and 180 rpm (growth experiments in polycarbonate Erlenmeyer flasks) or 350 rpm (growth experiments in 96-well plates) shaking. Maximum growth rates were calculated from three time points during the exponential phase of growth.

Construction of plasmids. For construction of the deletion plasmids pMW55, pMW56, and pMW61, the 600-bp regions upstream and downstream of the *pedS2* gene (*PP_2671*) or amino acid residue S178 in the *pedS2* gene (*PP_2671*) or *pedR2* gene (*PP_2672*) were amplified from genomic DNA of *P. putida* KT2440 using primers MWH90 to MWH93, MWH98 to MWH101, or MWH106 to MWH109 (Table 2). The two up- and downstream fragments and BamHI-digested pJOE6261.2 were then joined together using one-step isothermal assembly (47). Upon subsequent transformation of the constructs into *E. coli* BL21(DE3) cells, the correctness of the plasmids was confirmed by Sanger sequencing. Plasmids pJEM-[PedR2] and pJEM[PedR2^{D53A}] encoding PedR2 or PedR2 with mutated amino acid residue 53 (D→A) under a rhamnose-inducible promoter were ordered from an external source (Eurofins).

Strain constructions and isolation of suppressor mutants. The *pedS2* (*PP_2671*) and *pedR2* (*PP_2672*) negative mutants as well as the PedS2^{S178P} allele were constructed using a recently described system for markerless gene deletion in *P. putida* KT2440 (48). Briefly, the integration vectors harboring the up- and downstream regions of the target genes (pMW55 and pMW61) or the up- and downstream regions of the region to be mutated, including the desired S178P mutation (pMW56) were transformed into *P. putida* KT2440* and kanamycin-resistant (Kan^r) and 5-fluorouracil-sensitive (5-FU^s) clones were selected on LB Kan agarose plates. After incubation at 30°C for 24 h in LB medium without selection markers, clones that were 5-FU resistant (5-FU^r) and Kan^s were tested for successful gene deletion using primer pair MWH90/MWH93 or MWH106/MWH109 for the *pedS2* or *pedR2* gene, respectively. The presence of the underlying PedS2^{S178P} mutation was verified by Sanger sequencing after the *pedS2* gene of 5-FU^r and Kan^s clones was amplified using primer pair MWH85/MWH86. Δ *pedH* suppressor mutant strains were isolated from 25-ml liquid M9 cultures with 5 mM 2-phenylethanol as the sole source of carbon and energy supplemented with 10 µM La³⁺ upon >5-day incubation at 30°C and 180 rpm. Strains were passaged three times in LB agar plates and reevaluated for growth in liquid M9 medium supplemented with 5 mM 2-phenylethanol and 10 µM La³⁺. From cultures that showed growth with a lag phase similar to that of the wild-type KT2440* strain, the *pedS2* gene was amplified by PCR using primer pair M85/M86, and mutations were identified by Sanger sequencing.

To construct reporter strains for the analysis of *pedE* and *pedH* promoter activity in different genetic backgrounds, plasmids pUC18-mini-Tn7T-*pedE-lux-Gm* and pUC18-mini-Tn7T-*pedH-lux-Gm* (8) were co-electroporated with the helper plasmid pTNS2 into selected mutant strains of *P. putida* KT2440 (Table 1). Proper chromosomal integration of the mini-Tn7 element in gentamicin-resistant transformants was verified by colony PCR using P_{put-glmSDN} and P_{Tn7R} primers as described previously (49).

Reporter gene fusion assays. For quantitative measurement of *pedE* and *pedH* promoter activity, strains of *P. putida* harboring a Tn7-based *pedE-lux* or *pedH-lux* transcriptional reporter fusion were grown overnight in LB medium with gentamicin (15 µg · ml⁻¹), diluted to an OD₆₀₀ of 0.2 in fresh LB medium, and grown to an OD₆₀₀ of 0.6. The cells were then washed three times in M9 medium without a carbon source and finally adjusted to an OD₆₀₀ of 0.2 in M9 medium with 1 mM 2-phenylethanol. For luminescence measurements, 198 µl of a cell suspension was added to 2 µl of a 100 µM LaCl₃ solution

in white 96-well plates with a clear bottom (μ Clear; Greiner Bio-One). Microtiter plates were placed in a humid box to prevent evaporation and incubated at 28°C with continuous agitation (180 rpm), and light emission and OD₆₀₀ were recorded at regular intervals in an FLX-Xenius plate reader (SAFAS, Monaco) for 6 h. For both parameters, the background provided by the M9 medium was subtracted, and the luminescence was normalized to the corresponding OD₆₀₀. Experiments were performed with biological triplicates, and data are presented as the mean values with error bars representing the corresponding standard deviations.

Sequence identity determination. Protein sequence identities were determined based on amino acid sequence alignments of the proteins of interest generated using the Clustal Omega multiple-sequence alignment tool (50).

ACKNOWLEDGMENTS

The work of Matthias Wehrmann and Janosch Klebensberger was supported by an individual research grant from the Deutsche Forschungsgemeinschaft (DFG) (KL 2340/2-1). The work of Charlotte Berthelot and Patrick Billard was supported in part by Labex Resources 21 (ANR-10-LABX-21-01).

We thank Bernhard Hauer for his continuous support.

We declare that this research was conducted in the absence of any commercial or financial relationships that could be construed as a potential conflict of interest.

REFERENCES

1. Regenhardt D, Heuer H, Heim S, Fernandez DU, Strömpl C, Moore ERB, Timmis KN. 2002. Pedigree and taxonomic credentials of *Pseudomonas putida* strain KT2440. *Environ Microbiol* 4:912–915. <https://doi.org/10.1046/j.1462-2920.2002.00368.x>.
2. Wackett LP. 2003. *Pseudomonas putida* —a versatile biocatalyst. *Nat Biotechnol* 21:136–138. <https://doi.org/10.1038/nbt0203-136>.
3. Wu X, Monchy S, Taghavi S, Zhu W, Ramos J, van der Lelie D. 2011. Comparative genomics and functional analysis of niche-specific adaptation in *Pseudomonas putida*. *FEMS Microbiol Rev* 35:299–323. <https://doi.org/10.1111/j.1574-6976.2010.00249.x>.
4. Insam H, Seewald MSA. 2010. Volatile organic compounds (VOCs) in soils. *Biol Fertil Soils* 46:199–213. <https://doi.org/10.1007/s00374-010-0442-3>.
5. Peñuelas J, Asensio D, Tholl D, Wenke K, Rosenkranz M, Piechulla B, Schnitzler JP. 2014. Biogenic volatile emissions from the soil. *Plant Cell Environ* 37:1866–1891. <https://doi.org/10.1111/pce.12340>.
6. van Dam NM, Weinhold A, Garbeva P. 2016. Calling in the dark: the role of volatiles for communication in the rhizosphere, p 175–210. *In* Blande JD, Glinwood R (ed), *Deciphering chemical language of plant communication*. Springer International, Cham, Switzerland.
7. Mückschel B, Simon O, Klebensberger J, Graf N, Rosche B, Altenbuchner J, Pfannstiel J, Huber A, Hauer B. 2012. Ethylene glycol metabolism by *Pseudomonas putida*. *Appl Environ Microbiol* 78:8531–8539. <https://doi.org/10.1128/AEM.02062-12>.
8. Wehrmann M, Billard P, Martin-Meriadec A, Zegeye A, Klebensberger J. 2017. Functional role of lanthanides in enzymatic activity and transcriptional regulation of pyrroloquinoline quinone-dependent alcohol dehydrogenases in *Pseudomonas putida* KT2440. *mBio* 8:e00570-17. <https://doi.org/10.1128/mBio.00570-17>.
9. Toyama H, Mathews FS, Adachi O, Matsushita K. 2004. Quinohemoprotein alcohol dehydrogenases: structure, function, and physiology. *Arch Biochem Biophys* 428:10–21. <https://doi.org/10.1016/j.abb.2004.03.037>.
10. Anthony C. 2001. Pyrroloquinoline quinone (PQQ) and quinoprotein enzymes. *Antioxid Redox Signal* 3:757–774. <https://doi.org/10.1089/15230860152664966>.
11. Sarkar B. 2002. *Heavy metals in the environment*. CRC Press, Boca Raton, FL.
12. Fitriyanto NA, Fushimi M, Matsunaga M, Pertiwiingrum A, Iwama T, Kawai K. 2011. Molecular structure and gene analysis of Ce³⁺-induced methanol dehydrogenase of *Bradyrhizobium* sp. MAFF211645. *J Biosci Bioeng* 111:613–617. <https://doi.org/10.1016/j.jbiosc.2011.01.015>.
13. Chu F, Lidstrom ME. 2016. XoxF acts as the predominant methanol dehydrogenase in the type I methanotroph *Methylomicrobium buryatense*. *J Bacteriol* 198:1317–1325. <https://doi.org/10.1128/JB.00959-15>.
14. Good NM, Vu HN, Suriano CJ, Subuyuj GA, Skovran E, Martinez-Gomez NC. 2016. Pyrroloquinoline quinone ethanol dehydrogenase in *Methylobacterium extorquens* AM1 extends lanthanide-dependent metabolism to multicarbon substrates. *J Bacteriol* 198:3109–3118. <https://doi.org/10.1128/JB.00478-16>.
15. Pol A, Barends TRM, Dietl A, Khadem AF, Eygensteyn J, Jetten MSM, Op den Camp HJM. 2014. Rare earth metals are essential for methanotrophic life in volcanic mudpots. *Environ Microbiol* 16:255–264. <https://doi.org/10.1111/1462-2920.12249>.
16. Masuda S, Suzuki Y, Fujitani Y, Mitsui R, Nakagawa T, Shintani M, Tani A. 2018. Lanthanide-dependent regulation of methylotrophy in *Methylobacterium aquaticum* strain 22A. *mSphere* 3:e00462-17. <https://doi.org/10.1128/mSphere.00462-17>.
17. Vekeman B, Speth D, Wille J, Cremers G, De Vos P, Op den Camp HJM, Heylen K. 2016. Genome characteristics of two novel type I methanotrophs enriched from North Sea sediments containing exclusively a lanthanide-dependent XoxF5-type methanol dehydrogenase. *Microb Ecol* 72:503–509. <https://doi.org/10.1007/s00248-016-0808-7>.
18. Lv H, Sahin N, Tani A. 2018. Isolation and genomic characterization of *Novimethylophilus kurashikiensis* gen. nov. sp. nov., a new lanthanide-dependent methylotrophic species of *Methylophilaceae*. *Environ Microbiol* 20:1204–1223. <https://doi.org/10.1111/1462-2920.14062>.
19. Shiller AM, Chan EW, Joung DJ, Redmond MC, Kessler JD. 2017. Light rare earth element depletion during Deepwater Horizon blowout methanotrophy. *Sci Rep* 7:10389. <https://doi.org/10.1038/s41598-017-11060-z>.
20. Taubert M, Grob C, Howat AM, Burns OJ, Dixon JL, Chen Y, Murrell JC. 2015. XoxF encoding an alternative methanol dehydrogenase is widespread in coastal marine environments. *Environ Microbiol* 17:3937–3948. <https://doi.org/10.1111/1462-2920.12896>.
21. Farhan UI Haque M, Kalidass B, Bandow N, Turpin EA, DiSpirito AA, Semrau JD. 2015. Cerium regulates expression of alternative methanol dehydrogenases in *Methylosinus trichosporium* OB3b. *Appl Environ Microbiol* 81:7546–7552. <https://doi.org/10.1128/AEM.02542-15>.
22. Gu W, Semrau JD. 2017. Copper and cerium-regulated gene expression in *Methylosinus trichosporium* OB3b. *Appl Microbiol Biotechnol* 101:8499–8516. <https://doi.org/10.1007/s00253-017-8572-2>.
23. Vu HN, Subuyuj GA, Vijayakumar S, Good NM, Martinez-Gomez NC, Skovran E. 2016. Lanthanide-dependent regulation of methanol oxidation systems in *Methylobacterium extorquens* AM1 and their contribution to methanol growth. *J Bacteriol* 198:1250–1259. <https://doi.org/10.1128/JB.00937-15>.
24. Zheng Y, Huang J, Zhao F, Chistoserdova L. 2018. Physiological effect of XoxG(4) on lanthanide-dependent methanotrophy. *mBio* 9:e02430-17. <https://doi.org/10.1128/mBio.02430-17>.
25. Springer AL, Auman AJ, Lidstrom ME. 1998. Sequence and characterization of mxaB, a response regulator involved in regulation of methanol oxidation, and of mxaW, a methanol-regulated gene in *Methylobacterium extorquens* AM1. *FEMS Microbiol Lett* 160:119–124. <https://doi.org/10.1111/j.1574-6968.1998.tb12900.x>.
26. Springer AL, Morris CJ, Lidstrom ME. 1997. Molecular analysis of mxbD and mxbM, a putative sensor-regulator pair required for oxidation of

- methanol in *Methylobacterium extorquens* AM1. *Microbiology* 143: 1737–1744. <https://doi.org/10.1099/00221287-143-5-1737>.
27. Xu HH, Janka JJ, Viebahn M, Hanson RS. 1995. Nucleotide sequence of the *mxq* and *mxqE* genes, required for methanol dehydrogenase synthesis in *Methylobacterium organophilum* XX: a two-component regulatory system. *Microbiology* 141:2543–2551. <https://doi.org/10.1099/13500872-141-10-2543>.
 28. Skovran E, Palmer AD, Rountree AM, Good NM, Lidstrom ME. 2011. XoxF is required for expression of methanol dehydrogenase in *Methylobacterium extorquens* AM1. *J Bacteriol* 193:6032–6038. <https://doi.org/10.1128/JB.05367-11>.
 29. Chu F, Beck DAC, Lidstrom ME. 2016. MxaY regulates the lanthanide-mediated methanol dehydrogenase switch in *Methylomicrobium buryatense*. *PeerJ* 4:e2435. <https://doi.org/10.7717/peerj.2435>.
 30. Semrau JD, DiSpirito AA, Gu W, Yoon S. 2018. Metals and methanotrophy. *Appl Environ Microbiol* 84:e02289-17. <https://doi.org/10.1128/AEM.02289-17>.
 31. Arias S, Olivera ER, Arcos M, Naharro G, Luengo JM. 2008. Genetic analyses and molecular characterization of the pathways involved in the conversion of 2-phenylethylamine and 2-phenylethanol into phenylacetic acid in *Pseudomonas putida* U. *Environ Microbiol* 10:413–432. <https://doi.org/10.1111/j.1462-2920.2007.01464.x>.
 32. Parkinson JS. 2010. Signaling mechanisms of HAMP domains in chemoreceptors and sensor kinases. *Annu Rev Microbiol* 64:101–122. <https://doi.org/10.1146/annurev.micro.112408.134215>.
 33. Stock AM, Robinson VL, Goudreau PN. 2000. Two-component signal transduction. *Annu Rev Biochem* 69:183–215. <https://doi.org/10.1146/annurev.biochem.69.1.183>.
 34. Schobert M, Görisch H. 2001. A soluble two-component regulatory system controls expression of quinoprotein ethanol dehydrogenase (QEDH) but not expression of cytochrome *c*(550) of the ethanol-oxidation system in *Pseudomonas aeruginosa*. *Microbiology* 147: 363–372. <https://doi.org/10.1099/00221287-147-2-363>.
 35. Mern DS, Ha SW, Khodaverdi V, Gliese N, Görisch H. 2010. A complex regulatory network controls aerobic ethanol oxidation in *Pseudomonas aeruginosa*: indication of four levels of sensor kinases and response regulators. *Microbiology* 156:1505–1516. <https://doi.org/10.1099/mic.0.032847-0>.
 36. Van Kessel JC, Rutherford ST, Shao Y, Utria AF, Bassler BL. 2013. Individual and combined roles of the master regulators AphA and LuxR in control of the *Vibrio harveyi* quorum-sensing regulon. *J Bacteriol* 195: 436–443. <https://doi.org/10.1128/JB.01998-12>.
 37. Waters CM, Bassler BL. 2006. The *Vibrio harveyi* quorum-sensing system uses shared regulatory components to discriminate between multiple autoinducers. *Genes Dev* 20:2754–2767. <https://doi.org/10.1101/gad.1466506>.
 38. Milani M, Leoni L, Rampioni G, Zennaro E, Ascenzi P, Bolognesi M. 2005. An active-like structure in the unphosphorylated StyR response regulator suggests a phosphorylation-dependent allosteric activation mechanism. *Structure* 13:1289–1297. <https://doi.org/10.1016/j.str.2005.05.014>.
 39. Bourret RB, Hess JF, Simon MI. 1990. Conserved aspartate residues and phosphorylation in signal transduction by the chemotaxis protein CheY. *Proc Natl Acad Sci U S A* 87:41–45. <https://doi.org/10.1073/pnas.87.1.41>.
 40. Singh VS, Dubey AP, Gupta A, Singh S, Singh BN, Tripathi AK. 2017. Regulation of a glycerol-induced quinoprotein alcohol dehydrogenase by σ 54 and a LuxR-type regulator in *Azospirillum brasilense* Sp7. *J Bacteriol* 199:e00035-17. <https://doi.org/10.1128/JB.00035-17>.
 41. Rowland MA, Deeds EJ. 2014. Crosstalk and the evolution of specificity in two-component signaling. *Proc Natl Acad Sci U S A* 111:5550–5555. <https://doi.org/10.1073/pnas.1317178111>.
 42. Agrawal R, Sahoo BK, Saini DK. 2016. Cross-talk and specificity in two-component signal transduction pathways. *Future Microbiol* 11:685–697. <https://doi.org/10.2217/fmb-2016-0001>.
 43. Good NM, Walsler ON, Moore RS, Suriano C, Huff AF, Martinez-Gomez NC. 2018. Investigation of lanthanide-dependent methylotrophy uncovers complementary roles for alcohol dehydrogenase enzymes. *bioRxiv* <https://doi.org/10.1101/329011>.
 44. Nakagawa T, Mitsui R, Tani A, Sasa K, Tashiro S, Iwama T, Hayakawa T, Kawai K. 2012. A catalytic role of XoxF1 as La^{3+} -dependent methanol dehydrogenase in *Methylobacterium extorquens* strain AM1. *PLoS One* 7:e50480. <https://doi.org/10.1371/journal.pone.0050480>.
 45. Fitriyanto NA, Nakamura M, Muto S, Kato K, Yabe T, Iwama T, Kawai K, Pertiwiwinigrum A. 2011. Ce^{3+} -induced exopolysaccharide production by *Bradyrhizobium* sp. MAFF211645. *J Biosci Bioeng* 111:146–152. <https://doi.org/10.1016/j.jbiosc.2010.09.008>.
 46. Maniatis T, Sambrook J, Fritsch EF. 1982. *Molecular cloning: a laboratory manual*. Cold Spring Harbor Laboratory, Cold Spring Harbor, NY.
 47. Gibson DG. 2011. Enzymatic assembly of overlapping DNA fragments. *Methods Enzymol* 498:349–361. <https://doi.org/10.1016/B978-0-12-385120-8.00015-2>.
 48. Graf N, Altenbuchner J. 2011. Development of a method for markerless gene deletion in *Pseudomonas putida*. *Appl Environ Microbiol* 77: 5549–5552. <https://doi.org/10.1128/AEM.05055-11>.
 49. Choi KH, Gaynor JB, White KG, Lopez C, Bosio CM, Karkhoff-Schweizer RR, Schweizer HP. 2005. A Tn7-based broad-range bacterial cloning and expression system. *Nat Methods* 2:443–448. <https://doi.org/10.1038/nmeth765>.
 50. Sievers F, Wilm A, Dineen D, Gibson TJ, Karplus K, Li W, Lopez R, McWilliam H, Remmert M, Söding J, Thompson JD, Higgins DG. 2011. Fast, scalable generation of high-quality protein multiple sequence alignments using Clustal Omega. *Mol Syst Biol* 7:539. <https://doi.org/10.1038/msb.2011.75>.
 51. Jeske M, Altenbuchner J. 2010. The *Escherichia coli* rhamnose promoter rhaP BAD is in *Pseudomonas putida* KT2440 independent of Crp–cAMP activation. *Appl Microbiol Biotechnol* 85:1923–1933. <https://doi.org/10.1007/s00253-009-2245-8>.
 52. Winsor GL, Griffiths EJ, Lo R, Dhillon BK, Shay JA, Brinkman FSL. 2016. Enhanced annotations and features for comparing thousands of *Pseudomonas* genomes in the *Pseudomonas* genome database. *Nucleic Acids Res* 44:D646–D653. <https://doi.org/10.1093/nar/gkv1227>.
 53. Letunic I, Bork P. 2018. 20 years of the SMART protein domain annotation resource. *Nucleic Acids Res* 46:D493–D496. <https://doi.org/10.1093/nar/gkx922>.